IEEE Photonics Journal
An IEEE Photonics Society Publication

A Freeform Mirror Design of Uniform Illumination in Streetlight From a Split Light Source

Volume 10, Number 4, August 2018

Cheng-Mu Tsai
Bo-Xiang Wang

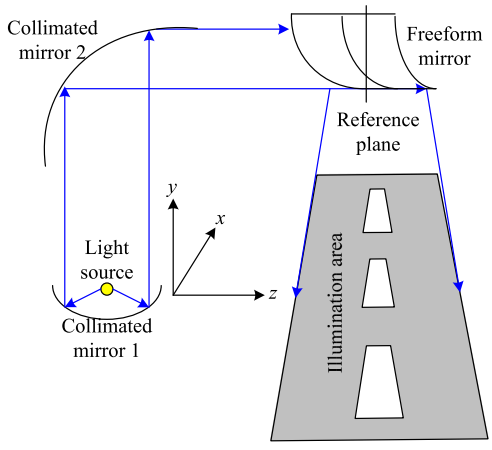

DOI: 10.1109/JPHOT.2018.2860796
1943-0655

A Freeform Mirror Design of Uniform Illumination in Streetlight From a Split Light Source

Cheng-Mu Tsai and Bo-Xiang Wang

Graduate Institute of Precision Engineering, National Chung Hsing University, Taichung city 402, Taiwan, R.O.C.

DOI:10.1109/JPHOT.2018.2860796

Manuscript received February 19, 2018; revised July 23, 2018; accepted July 24, 2018. Date of publication July 27, 2018; date of current version August 13, 2018. This work was supported by the Ministry of Science and Technology of the Republic of China under Contracts MOST 106-2221-E-005-055, MOST 106-2622-E-005-007-CC3, and MOST 106-2622-E-005-018-CC2. Corresponding author: Cheng-Mu Tsai (e-mail: jmutsai@email.nchu.edu.tw).

Abstract: A streetlight with a split light source is presented to construct a freeform mirror for converting a certain light distribution into uniform illumination. It is easy to maintain the proposed streetlight because the light sources are placed at the bottom of the lamppost. Two collimated mirrors are employed to allow the rays to travel a long distance without much loss of power. There are 400 × 400 pieces of area divided at a reference plane (RP), a freeform mirror (FM) and an illumination area (IA). According to light distribution, a method is proposed to evaluate the equal luminance at each RP-divided area. Such equal luminance is expected to develop the FM to reflect rays into the IA with uniform illumination. The simulation results show that average illumination is 20.6 lx in the required area with 90% power efficiency, 85.9% uniformity, and lower glare.

Index Terms: Light-emitting diodes, Illumination design, Nonimaging optics.

1. Introduction

With their small size, high energy efficiency and long lifetime, light-emitting diodes (LEDs) have become a very popular light source with various applications. Many streetlights employed LEDs as their light source. Lighting equipment with LEDs usually employs a secondary lens to convert their light distribution into a specific display over a specific area. Such a secondary lens [1]–[6] is installed in streetlights to make them illuminate their area more uniformly and with less glare.

Among the secondary lens constructions, one structure, called the freeform surface [7]–[14], is widely considered in creating a secondary lens to meet the specifications. Common secondary lens design involves an LED chip with rotationally symmetrical light distribution inside the lens structure. Some mapping schemes [7], [8] apply Snell's law to create a freeform surface which converts the light distribution of the LED to a specific distribution. Most of the rays emitted from the LED chip are refracted through the freeform surface toward the prescribed directions, but some radiative rays may deviate from the prescribed direction to induce the effect of glare. With a combination of reflective surfaces, however, the deviant rays can be controlled to lower the level of effect from the secondary lens [2], [6].

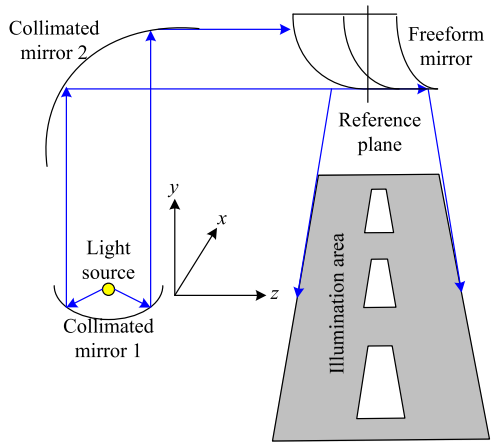

Fig. 1. The architecture of a streetlight with split light source.

A popular method [13] applied the Hamiltonian theory in Cartesian oval representation for the freeform optics design of illumination system. Compared with the refraction type, the freeform reflector can be negligible in the chromatic aberration and it is more flexible for the reflector to control the optical radiation with collimation into desired direction. R. Zhu *et al.* [14] applied the ellipsoid approach based on the intersection calculation to improve the speed and accuracy of the freeform reflector design. Such a design is only to concern the light source inside the freeform reflector, which would limit the location of the light source. Instead of the single mirror configuration, the proposed three-mirror configuration could allow the light source placed at the desired position so that it is more flexible for the illumination system with split light source.

Most streetlights with LEDs place the secondary lens for illumination at the top of the lamppost. But this means that maintenance workers must climb to the top of the lamppost to replace LEDs when they break, which is inconvenient. In this paper, however, a streetlight with split light sources is proposed to make maintenance easier. Using the concept of split light sources, the LEDs can be placed at the bottom of streetlight for easy replacement. Some collimated lenses or mirrors are employed to allow the rays to travel the long distance from the bottom to the secondary lens; they then provide uniform illumination in the desired area. Instead of the secondary lens, in this paper we construct a freeform mirror to bring uniformity to the light distribution with rectangle region.

A streetlight with four LEDs is constructed in the required area to estimate the uniformity and power efficiency. As a result, the illumination area receives 20.6 lx average illumination with 85.9% uniformity, 90% power efficiency, and lower glare. The paper is organized as follows. Section 2 describes how to construct a streetlight with a split light source. The simulation results are discussed in Section 3. Section 4 concludes this paper.

2. Construction of Streetlight With Split Light Source

It is more convenient to replace a light source which is at the bottom of a streetlight. Fig. 1 shows the architecture of a streetlight using a split light source. It consists of light sources, two collimated mirrors (CMs) and a freeform mirror (FM). The light sources are placed at the base of the streetlight for easy maintenance. Placing the light sources at the focal point of the CMs leads the rays to propagate in collimation with less loss of power. The second CM steers the rays into the FM and makes the rays more collimated. Regarding a certain light distribution from the reference plane (RP), the FM is responsible for providing uniform illumination of the illumination area (IA). The streetlight is always built with a pipe. The 1st CM of course is installed inside of the pipe so that the dust, rain and snow could be minimum effect for the operation of the 1st CM.

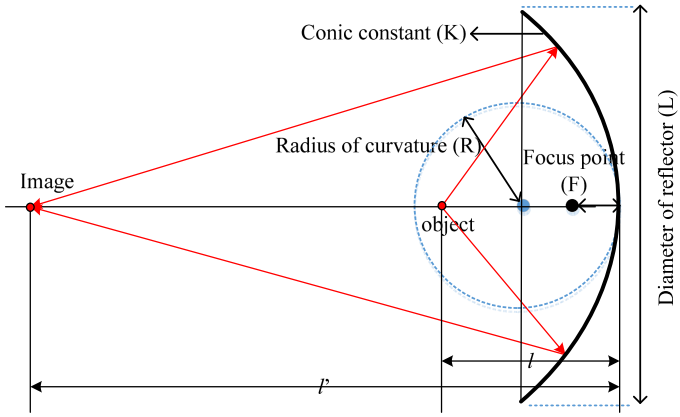

Fig. 2. The structure of the first collimated mirror.

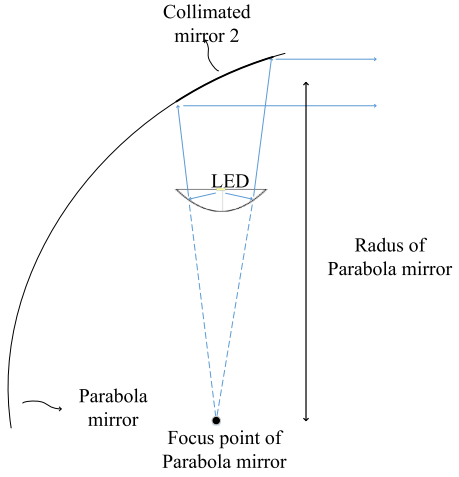

Fig. 3. The construction of the second collimated mirror.

2.1 Collimated Mirror Design

The rays from the split light sources need to reach the top of the streetlight and be reflected by the FM onto the IA. A CM is applied to make the rays travel from the bottom to the top of the streetlight. Fig. 2 shows the structure of the first CM. The light source is placed at the focal point of the mirror to collimate the rays according to

$$1/l' - 1/l = 1/f \tag{1}$$

where l and l' are the object and image distances, respectively. The f is the effective focal length (EFL). Given the radius R, the EFL for the mirror is $R/2$. Moreover, an aspherical surface with conic constant $K = -1$ is employed to suppress spherical aberration. When an object is placed at the focus point, the image distance l' is at infinity to make the ray collimation.

The main function of the second CM is to reflect the collimated rays onto the FM. Since the FM is based on the collimated ray to construct for making uniformity on the road, the rays propagate to the FM are required to be collimated. However, the LED is not a point light source, which induces small divergence for the reflective rays from the first CM. The second CM can also be designed to improve the collimation, as shown in Fig. 3. We expect that an intersection point can be generated from the two outmost divergence rays. Such a point is treated as the focal point of the second CM. The radius of the CM is determined from a line that runs from the focal point passing through the LED to a reflective point in the second CM, as shown in Fig. 3. The calculated parameters are

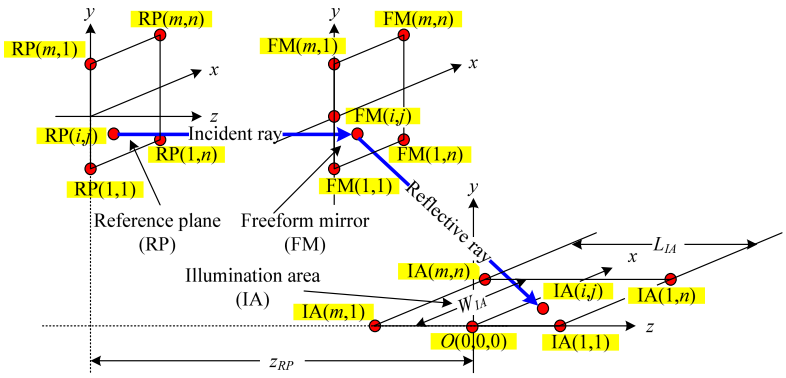

Fig. 4. The freeform mirror design scheme.

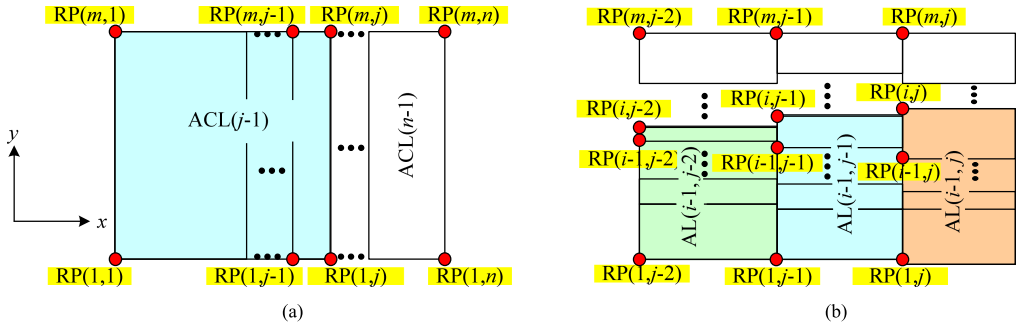

Fig. 5. The luminance average scheme. (a) for a column (b) for a grid area.

applied to construct the second CM to not only enhance the collimation but also to reflect the rays onto the FM.

2.2 Freeform Mirror Design Based on Non-Uniform Light Distribution

The two CMs are used to conduct the rays propagated to the FM to illuminate the required area with uniform distribution. The rays from the second CM are collimated again to propagate to the RP that is placed around the FM to estimate the light distribution for designing the FM with uniform illumination. The structure of the FM is related to the RP with a certain light distribution and the IA, as shown in Fig. 4. There are $m \times n$ points arranged at the RP, FM and IA to divide individually into $(m-1) \times (n-1)$ areas. Each area at the RP has the same luminance but it is the same size as the IA. A mapping algorithm is planned to cast the luminance of area (i, j) from the RP into the specific area (i, j) of the IA through the FM to create uniform illumination at the IA. Fig. 4 shows the incident ray from the point (i, j) of the RP is reflected by the point (i, j) of the FM, then travels toward the point (i, j) of the IA.

Let point $(x_{FM(i,j)}, y_{FM(i,j)}, z_{FM(i,j)})$ at the FM(i, j) be the same as point $(x_{RP(i,j)}, y_{RP(i,j)}, z_{RP(i,j)})$ of the RP(i, j), except in the z direction so as to adjust the surface to reflect the ray into the specific area of the IA. The $z_{RP(i,j)}$ is a constant z_{RP}; that is, the distance from the original O to the streetlight in z-direction, as shown in Fig. 4. According to the light distribution at the RP, the positions of the points can be found to make the same luminance at the divided area. Fig. 5 shows the scheme for averaging the luminance at the RP. There are $(n-1)$ column areas divided in the x-direction, based on the luminance distribution $L(x, y)$, as shown in Fig. 5(a). Each column area is allocated the average column luminance (ACL) as follows:

$$\mathrm{ACL} = \frac{\int_{y_{RP(1,1)}}^{y_{RP(m,1)}} \int_{x_{RP(1,1)}}^{x_{RP(1,n)}} L(x, y)dxdy}{(n-1)} \tag{2}$$

The accumulated luminance from the first column area to the $(j-1)$th column area is

$$\mathrm{ACL}\,(j-1)=\int_{x_{RP(1,1)}}^{x_{RP(1,j)}}\int_{y_{RP(1,1)}}^{y_{RP(m,1)}}L\,(x,y)dydx=(j-1)\times\mathrm{ACL} \tag{3}$$

Using Eq. (3), we can find the $x_{RP(1,j)}$ to average the column luminance at the RP. The position of point RP(i, j) at the x-direction is set to $x_{\mathrm{RP}(i,j)}=x_{RP(1,j)}$ for $i=2,\ldots,m$ to give the same luminance ACL for each column area. There are $m-1$ grid areas for each column, as shown in Fig. 5(b). The grid areas must also have the same average luminance (AL); that is,

$$\mathrm{AL}=\mathrm{ACL}/\,(m\;-\;1) \tag{4}$$

The accumulated luminance from the first grid to the $(i-1)$th grid at the $(j-1)$th column is

$$\mathrm{AL}\,(i-1,\;j-1)=\int_{y_{RP(1,j-1)}}^{y_{RP(i,j-1)}}\int_{x_{RP(1,j-1)}}^{x_{RP(1,j)}}L\,(x,y)dxdy=(i-1)\times\mathrm{AL} \tag{5}$$

Using the Eq. (5), the $y_{RP(i,j-1)}$ can be found to average the grid luminance at column area $(j-1)$. Note that the $y_{RP(i,j-1)}$ could not be the same as the $y_{RP(k,j-1)}$ and $y_{RP(i,l-1)}$ for $k=2,\ldots,m-1$, $k\neq i$ and $l=2,..,n-1, l\neq j$.

For uniform illumination, the IA must be divided equally into $(m-1)\times(n-1)$ areas to receive the same luminance. Suppose the IA with width W_{IA} and length L_{IA} at x- and z-direction, as shown in Fig. 4. The point $(x_{\mathrm{IA}(i,j)},\ y_{\mathrm{IA}(i,j)},\ z_{\mathrm{IA}(i,j)})$ of the IA(i, j) can be represented as

$$x_{\mathrm{IA}(i,j)}=W_{IA}\,(j\;-\;1)\,/\,(n\;-\;1)\ \text{ for } j=1,\ldots,n \tag{6a}$$

$$y_{\mathrm{IA}(i,j)}=0, \tag{6b}$$

$$z_{\mathrm{IA}(i,j)}=L_{IA}/2-L_{IA}\,(i\;-\;1)\,/\,(m\;-\;1)\ \text{ for } i=1,\ldots,m \tag{6c}$$

All the points at the RP, FM and IA can be found by using Equations (3), (5) and (6), except the $z_{\mathrm{FM}(i,j)}$. Since the two mirrors have collimated rays into the RP already, the incident vector between points RP(i, j) and FM(i, j) can be approached as $\mathbf{I}(i,j)=[\,0\,0\,1\,]$. After the FM reflection, the rays would propagate toward the IA with the reflective vector as follows:

$$\mathbf{R}(i,j)=\frac{[x_{IA(i,j)}y_{IA(i,j)}z_{IA(i,j)}]-[x_{FM(i,j)}y_{FM(i,j)}z_{FM(i,j)}]}{\left\|[x_{IA(i,j)}y_{IA(i,j)}z_{IA(i,j)}]-[x_{FM(i,j)}y_{FM(i,j)}z_{FM(i,j)}]\right\|} \tag{7}$$

where the operator || || is the norm for normalizing the $\mathbf{R}(i, j)$ so as to be a unit vector. Given the incident vector $\mathbf{I}(i, j)$ and reflective vector $\mathbf{R}(i, j)$, the normal vector $\mathbf{N}(i, j)$ can be represented as

$$\mathbf{N}(i,j)=[a_{(i,j)}\ b_{(i,j)}\ c_{(i,j)}]=\frac{\mathbf{I}(i,j)-\mathbf{R}(i,j)}{\sqrt{2(1+\mathbf{I}(i,j)\cdot\mathbf{R}(i,j))}} \tag{8}$$

The normal vector $\mathbf{N}(i, j)$ is applied to find the $z_{\mathrm{FM}(i+1,\,j)}$ and $z_{\mathrm{FM}(i,\,j+1)}$ of the next adjacent point.

The point inside the plane FM except for the bolder boundary would lead to two points with the same normal vector, i.e., creating the vertical and horizontal points. Fig. 6 shows the relationship between point FM_V(i, j) and the adjacent points FM_V$(i+1, j)$ and FM_H$(i, j+1)$. Let points FM_V(i, j), FM_V$(i+1, j)$ and FM_H$(i, j+1)$ form a plane with normal vector $\mathbf{N}(i, j)$. According to the plane equation, we know

$$a_{(i,j)}\left[x_{\mathrm{FM\_V}(i+1,j)}-x_{\mathrm{FM\_V}(i,j)}\right]+b_{(i,j)}\left[y_{\mathrm{FM\_V}(i+1,j)}-y_{\mathrm{FM\_V}(i,j)}\right]+c_{(i,j)}\left[z_{\mathrm{FM\_V}(i+1,j)}-z_{\mathrm{FM\_V}(i,j)}\right]=0 \tag{9a}$$

and

$$a_{(i,j)}\left[x_{\mathrm{FM\_H}(i,j+1)}-x_{\mathrm{FM\_V}(i,j)}\right]+b_{(i,j)}\left[y_{\mathrm{FM\_H}(i,j+1)}-y_{\mathrm{FM\_V}(i,j)}\right]+c_{(i,j)}\left[z_{\mathrm{FM\_H}(i,j+1)}-z_{\mathrm{FM\_V}(i,j)}\right]=0 \tag{9b}$$

Using Equation (9), we can determine the zFM_V$(i+1, j)$ and zFM_H$(i,\ j+1)$ to construct the FM.

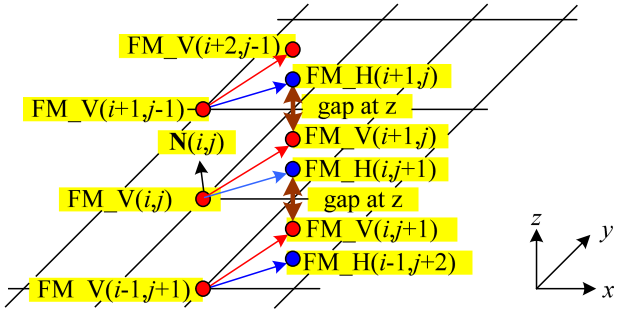

Fig. 6. The point derivation of the freeform mirror.

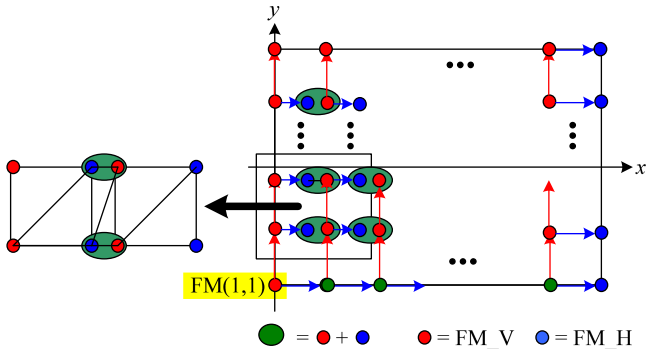

Fig. 7. The construction plan of the freeform mirror.

Note that the points FM(i, j), FM_V(i, j) and FM_H(i, j) have the same coordinates except in the z direction. Therefore, there is a gap in the z-direction for points FM_V($i+1, j$) and FM_H($i+1, j$), as shown in Fig. 6. Fig. 7 illustrates how the FM is constructed. The initial point is FM(1, 1), which can create FM_V(2, 1) and FM_H(1, 2). No vertical points are created at the bottom bolder boundary, so that point FM_V(1, j) is set to be FM_H(1, j) to continue the FM construction. The top bolder boundary is allowed only by the vertical points, while the rightmost bolder boundary can be constructed only by the horizontal points. As we know, three points can construct a plane. All the constructed planes are connected appropriately to form the final discrete FM, as shown in Fig. 7.

3. Simulation Result and Discussion

An LED with model XLamp XHP35 HI from Cree Corporation [15] was employed in the design of the proposed streetlight. Its size is $3.45 \times 4.35\,\text{mm}^2$. The optical flux is about 1400 lm. The number of rays tracing is set to 10^6 for each LED. Fig. 8 shows the illumination and intensity for the LED model XHP35 HI. As we see, the luminous intensity approaches Lambertian distribution. Since the illumination is required to be 4500 lm for the required area $25 \times 10\,\text{m}^2$, it is necessary to employ four LEDs to approach 5600 lm in order to satisfy the specification of the streetlight. Each LED associates with two CMs to realize the collimation. The LEDs are placed at 1.5 m from the ground for easy replacement. The height of the streetlight is the standard 6 m. The second CMs are placed at a height of 6 m not only to collimate the light again but also to reflect the rays into the FM. Fig. 9 shows the relative positions for the CMs, RP and FM.

When placing the light source at the focal point, the collimation was related to the radius of the mirror and the size of the light source. Three radiuses (i.e., 75 mm, 100 mm, and 125 mm) were investigated to find an appropriate one for constructing the first CM. The distance between the first CM and the second CM was set to 4.5 m so that a detector was placed 4.5 m away from the first CM to evaluate the collimation. Fig. 10 shows the luminous intensity for radiuses of 75 mm,

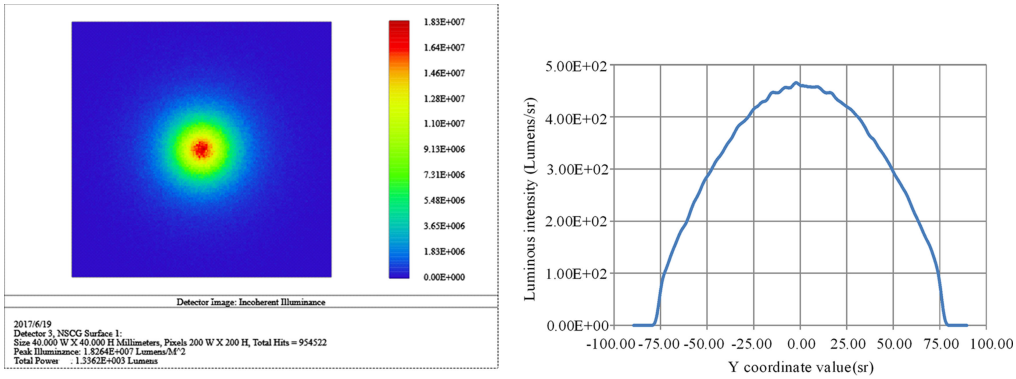

Fig. 8. LED with model XHP35 HI for (a) incoherent illumination (b) luminous intensity.

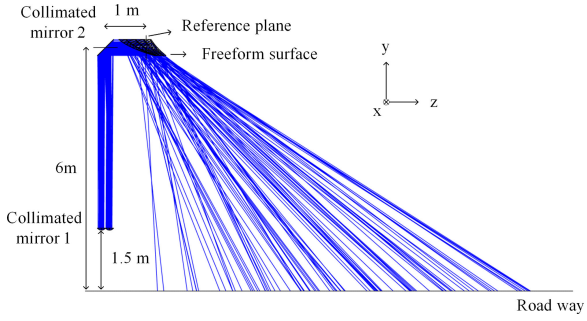

Fig. 9. The relative positions for the CMs, RP and FM.

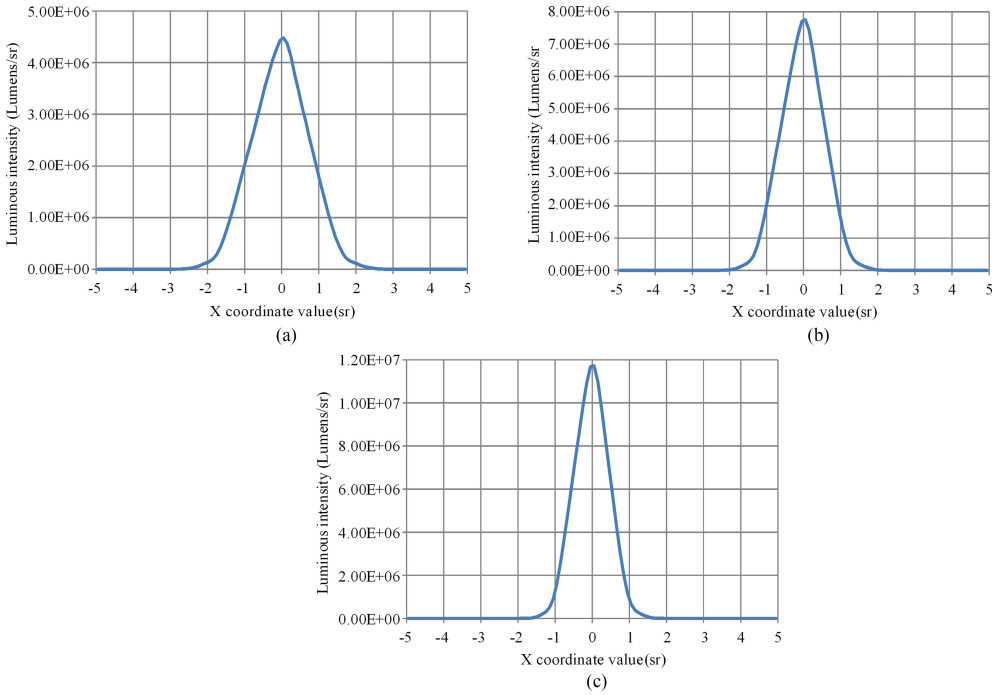

Fig. 10. The luminous intensity from the first CM for a radius of (a) 75 mm (b) 100 mm (c) 125 mm.

TABLE 1
The Datasheet of the First Collimated Mirrors For the Three Radiuses

Radius (mm)	Aperture (mm)	Divergence (sr)
75	150x150	2.5
100	200x200	2
125	250x250	1.5

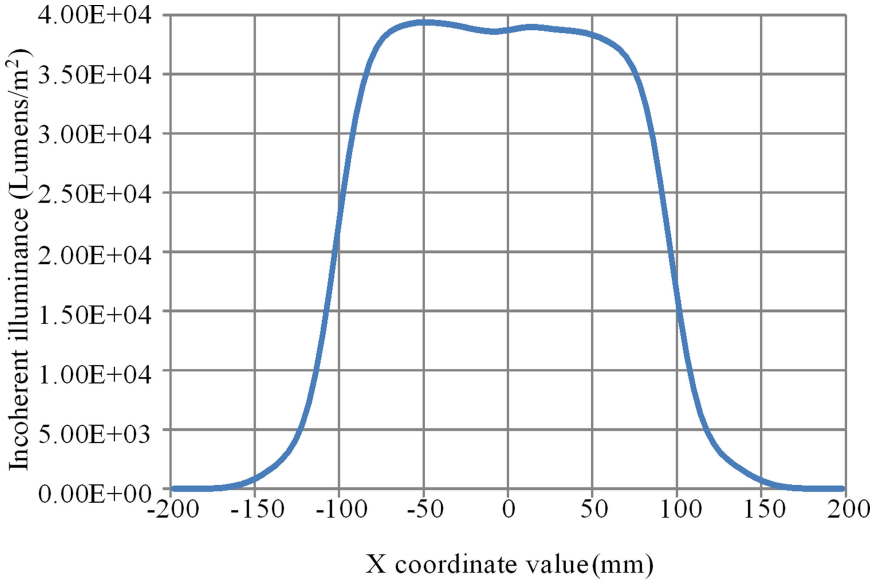

Fig. 11. Cross section of the illumination for one LED.

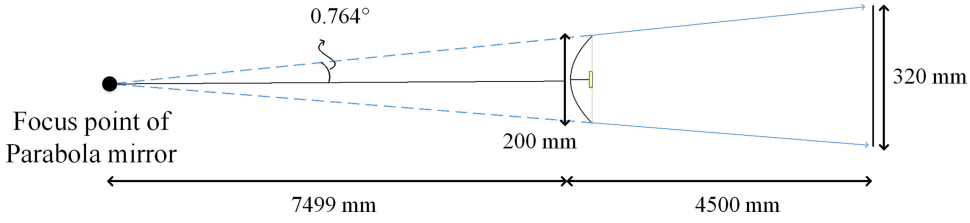

Fig. 12. Derivation of the second collimated mirror.

100 mm and 125 mm. The results show that radius 125 mm had a better collimation than the others, as shown in Table 1. However, a larger space was required for a radius of this size. Regarding the collimation and space limit, a radius of 100 mm was considered to be applicable for the first CM.

Although the first CM was designed to make the rays collimated, the non-point light source would have caused the rays between the RP and the FM to be uncollimated. Moreover, the rays must be redirected to the FM to provide uniform illumination over the specific area. The second CM is responsible for collimating the rays again and reflecting the rays onto the FM. Fig. 11 shows a cross section of incoherent illuminance for the first CM with a radius of 100 mm. The illumination area at the x-direction extended roughly from -160 mm to 160 mm, which indicated divergence angle of 0.764°, as shown in Fig. 12. Because the diameter of the first CM was set to 200 mm, a point light source can be imaged at the 7499 mm ahead of the first CM. Therefore, the radius of the second CM was set to 11999 mm. Its area was set to 200×200 mm^2 to receive most of the rays from the first CM.

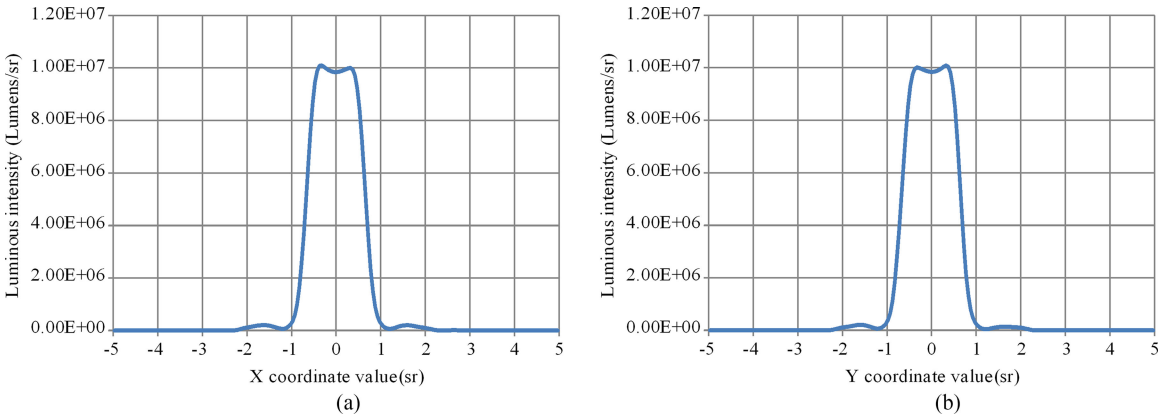

Fig. 13. The luminous intensity of the reference plane for (a) a cross section at the x-direction (b) a cross section at the y-direction.

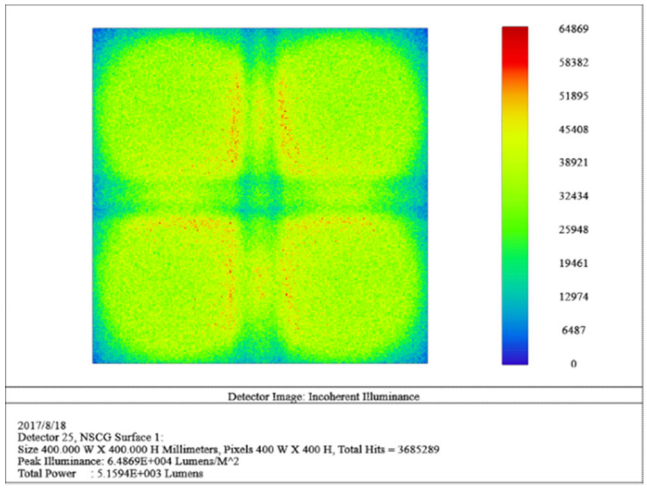

Fig. 14. The incoherent illumination at the reference plane.

To estimate the optical information, the rays reflected by the two CMs would have arrived at the RP. The luminance intensity is shown in Fig. 13. As we see, the divergence angle is improved from 2° (see Fig. 10) to around 1° under the radius of the first CM being 100 mm. Fig. 14 shows the incoherent illumination at the RP. Such an optical distribution is expected to build the FM to complete the uniform illumination in the specific area. There are $(m-1) \times (n-1)$ pieces of rectangle area partitioned to allocate the same luminance at the RP. The illumination region is also divided into $(m-1) \times (n-1)$ pieces of equal area in the street. In this research, an FM with 400×400 pieces was constructed to conduct the rays from the RP (400×400 mm^2) to the specific area (10×25 m^2) of the street.

As expected, the FM with 400×400 pieces was able to transform a certain optical distribution from the RP into the IA with more uniform illumination, as shown in Fig. 15. The power efficiency was 90%. However, the illumination area shown in Fig. 15 was slightly irregular. Consequently, a staggered arrangement of streetlights may be the best choice. Fig. 16 shows the illumination gained by placing three streetlights in a staggered arrangement. Following the IESNA regulation [16], the test region was set to 2.5×2.5 m^2, as shown in Fig. 16. The maximum, average and minimum luminances were respectively 22.1 lx, 20.6 lx and 17.7 lx, which indicates 85.9% uniformity and corresponds to the requirement of the IESNA.

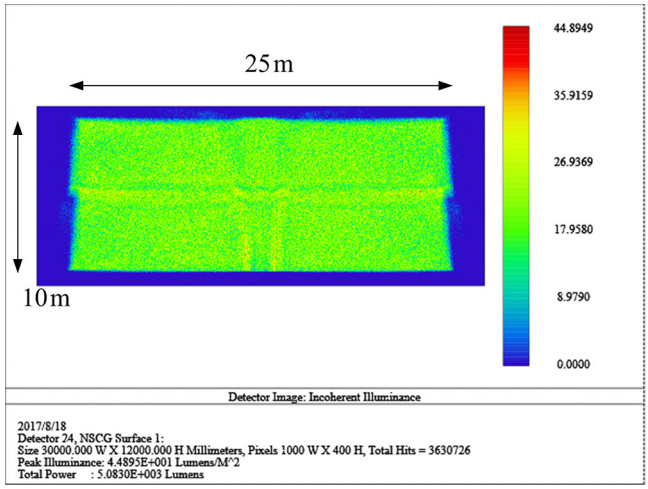

Fig. 15. Illumination of the illumination area by a streetlight alone.

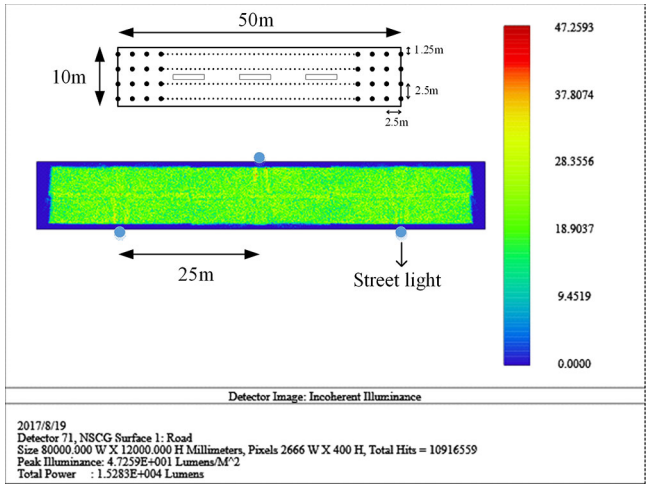

Fig. 16. Illumination of the illumination area by a staggered arrangement of streetlights.

A traditional image lens is to mount a multiple of lens elements into a metal barrel [17]. Current precision is possible to promise 10 μm [17] for the optical system and the precision will be more accurate in the future. The proposed streetlight can be assembled by using the lens barrel assembly [17]. A tolerance analysis is estimated for the proposed streetlight, as shown in Fig. 17. In this paper, the position of light source is more sensitive than the other lens elements. Fig. 17(a) shows that there is about $\pm$500 μm tolerance for the LED displacement under the IESNA uniformity requirement above 33%. However, the second CM and the FM position allow at least $\pm$30 mm tolerance, as shown in Fig. 17(b) and (c). As a result, the proposed streetlight can satisfy the fabrication requirement in precision.

Another issue we could concern about is that some parts like the PCB or the heat sink would block the partial optical flux at the aperture. The dimension of the heat sink is 16 mm in diameter for the proposed light source. Fig. 18 shows the illumination simulation with the heat sink in a staggered arrangement of streetlights. Using the FM same as previous one receives 85.9% uniformity, as shown in Fig. 18(a). Since the uniformity of the proposal is according to the light distribution of the reference plane to design the FM, the light distribution of the RP is also influenced by some blocking. Therefore, the light distribution with the blocking effect can be considered in FM design to make the uniform illumination in the target. A new FM is re-built according to the light distribution of the

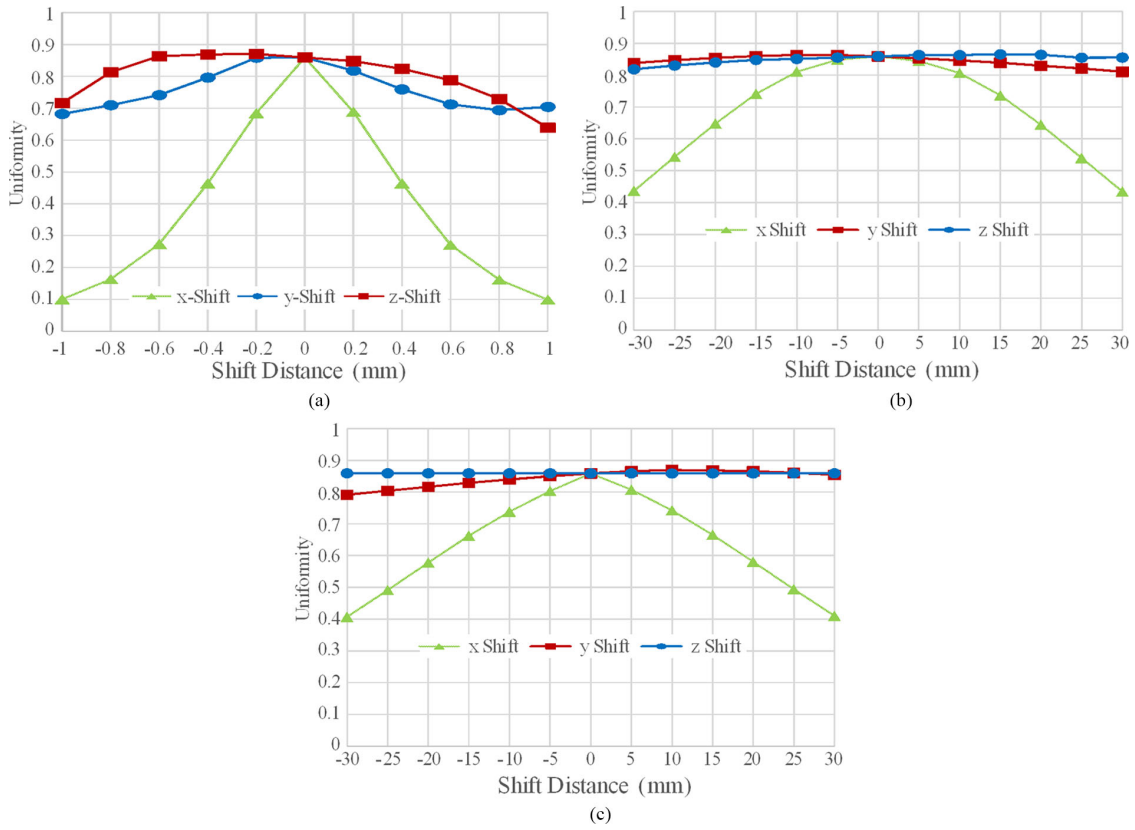

Fig. 17. The relation between the uniformity and (a) the position of the LED (b) the second CM (c) the FM.

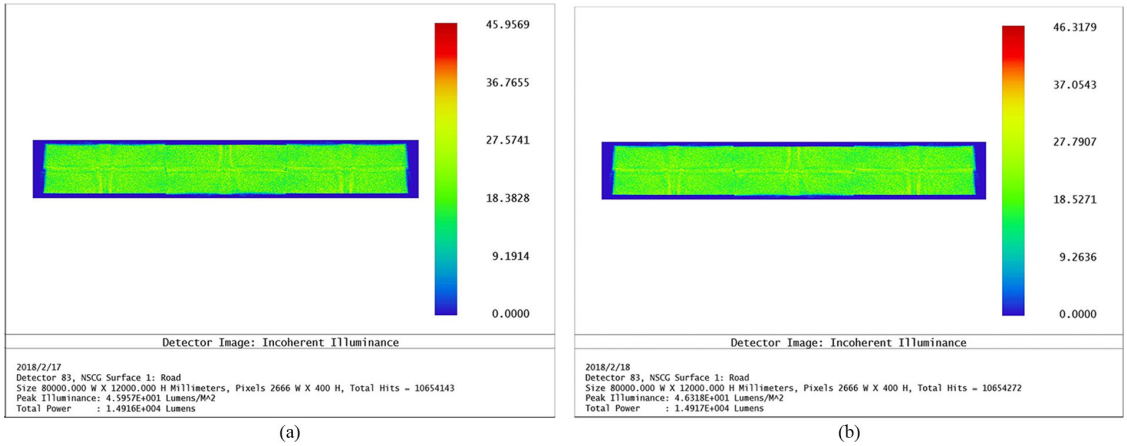

Fig. 18. Illumination of the illumination area in a staggered arrangement of streetlights by (a) using previous FM (b) building a new FM.

RP with the heat sink. The uniformity is about 86% in a staggered arrangement of streetlights, as shown in Fig. 18(b). If someone concerns about the blocking optical flux at the aperture, a refractive lens with collimation can replace to make the same function of the 1st CM.

4. Conclusion

A streetlight based on a split light source is proposed to reduce the difficulty of maintenance. It is more convenient to replace the light sources if they are at the base of the streetlight. However, the illumination requires the rays to be propagated from the top of the streetlight to the IA. Using two CMs steers the rays from the light source onto the FM to complete the uniform illumination of the IA. With 400 $\times$ 400 pieces of area partitions in the RP, FM and IA, uniform illumination is realized on the basis of light distribution of the RP to allocate equal luminance to each piece, constructing the FM. As a result, the proposed streetlight can reach an average illumination of 20.6 lx in the IA, with 90% power efficiency, 85.9% uniformity and lower glare.

References

[1] J.-W. Pan, S.-H. Tu, W.-S. Sun, C.-M. Wang, and J.-Y. Chang, "Integration of non-lambertian LED and reflective optical element as efficient street lamp," *Opt. Exp.*, vol. 18, no. 13, pp. A221–A230, 2010.
[2] J. Jiang, S. To, W. B. Lee, and B. Cheung, "Optical design of a freeform TIR lens for LED streetlight," *Optik*, vol. 121, no. 19, pp. 1761–1765, 2010.
[3] Z. Feng, Y. Luo, and Y. Han, "Design of LED freeform optical system for road lighting with high luminance/illuminance ratio," *Opt. Exp.*, vol. 18, no. 21, pp. 22020–22031, Oct. 2010.
[4] S. Wang, K. Wang, F. Chen, and S. Liu, "Design of primary optics for LED chip array in road lighting application," *Opt. Exp.*, vol. 19, no. 14, pp. A716–A724, 2011.
[5] H.-C. Chen, J.-Y. Lin, and H.-Y. Chiu, "Rectangular illumination using a secondary optics with cylindrical lens for LED street light," *Opt. Exp.*, vol. 21, no. 3, pp. 3201–3212, 2013.
[6] M.-F. Lai, Y.-C. Chen, N. D. Q. Anh, T.-Y. Chen, H.-Y. Ma, and H.-Y. Lee, "Design of asymmetric freeform lens for low glared LED street light with total internal reflection," *Opt. Exp.*, vol. 24, no. 2, pp. 1409–1415, 2016.
[7] K. Wang, S. Liu, F. Chen, Z. Qin, Z. Liu, and X. Luo, "Freeform LED lens for rectangularly prescribed illumination," *J. Opt. A, Pure Appl. Opt.*, vol. 11, no. 10, Oct. 2009, Art. no 105501.
[8] J.-. Chen, T.-Y. Wang, K.-L. Huang, T.-S. Liu, M.-D. Tsai, and C.-T. Lin, "Freeform lens design for LED collimating illumination," *Opt. Exp.*, vol. 20, no. 10, pp. 10984–10995, 2012.
[9] Z.-M. Zhu, H. Liu, and S.-M. Chen, "The design of diffuse reflective free-form surface for indirect illumination with high efficiency and uniformity," *IEEE Photon. J.*, vol. 7, no. 3, Jun. 2015, Art. no. 1600510.
[10] N. Wu, L. Feng, and A. Yang, "Localization accuracy improvement of a visible light positioning systembased on the linear illumination of LED sources," *IEEE Photon. J.*, vol. 9, no. 5, Oct. 2017, Art. no. 7905611.
[11] C.-C. Sun *et al.*, "Design of LED street lighting adapted for free-form roads," *IEEE Photon. J.*, vol. 9, no. 1, Feb. 2017, Art. no. 8200213.
[12] S. Babadi, R. Ramirez-Iniguez, T. Boutaleb, and T. Mallick, "Performance comparison of a freeform lens and a CDTIRO whencombined with an LED," *IEEE Photon. J.*, vol. 9, no. 5, Oct. 2017, Art. no. 6501008.
[13] D. Michaelis, P. Schreiber, and A. Brauer, "Cartesian oval representation of freeform optics in illumination systems," *Opitcs Lett.*, vol. 36, no. 6, pp. 918–920, 2011.
[14] R. Zhu, Q. Hong, H. Zhang, and S. T. Wu, "Freeform reflectors for architectural lighting," *Opt. Exp.*, vol. 23, no. 25, pp. 31828–31837, 2015.
[15] XLamp XHP35 High Intensity, 2017. [Online]. Available: http://www.cree.com/led-components/products/xlamp-leds-discrete/xlamp-xhp35-high-intensity
[16] *The IESNA Lighting Handbook: Reference and Application*, 9th ed., Illuminating Eng. Soc. North Amer., New York, NY, USA, 2000.
[17] K. Schwertz and J. Burge, *Field Guide to Optomechanical Design and Analysis*, vol. FG26. Bellingham, WA, USA: SPIE Press, 2012, pp. 57–61.